

Intelligent Control of a Prosthetic Ankle Joint

Anh Mai and Sesh Commuri

School of Electrical and Computer Engineering, University of Oklahoma, Norman, Oklahoma, U.S.A.

Keywords: Intelligent Control, Prosthetic Foot, Optimization.

Abstract: The ability to control the prosthetic ankle joints of below-knee amputees is a challenging problem due to the lack of adequate mathematical models, the variations in the gait in response to the environment, sensor noise, and unknown intent of users. Artificial ankle joints are required to exhibit variable stiffness based on the gait and aid in locomotion as well as stability of the individual. It is desirable for control strategies for such ankle joints to adapt in real-time to any variations in the gait, have robust performance, and optimize specified performance indices relating to efficiency of the gait. In this paper, we investigate the potential of Direct Neural Dynamic Programming (DNDP) method for learning the gait in real-time and in generating control torque for the ankle joint. The residual limb is first represented by a link-segment model and the kinematic patterns for the model are derived from human gait data. Then augmented training rules are proposed to implement the DNDP-based control to generate torque which drives the prosthetic ankle joint along the designed kinematic patterns. Numerical results show that the DNDP controller is able to maintain stable gait with robust tracking and reduced performance cost in spite of measurement/actuator noises and variations in walking speed.

1 INTRODUCTION

Current ankle/foot prostheses are primarily passive devices whose performance cannot be adapted or optimized to meet the requirements of different users. Further, such devices cannot provide the rigidity, as well as the flexibility and power similar to that of a human foot. The adverse consequences of wearing less functioning prosthetic feet include asymmetric gait, increased metabolic consumption, limited blood flow, instability, and pain. In the long-term, the amputees, especially ones with diabetes, might have to undergo hip replacement procedure and use wheel-chair on a daily basis.

The lack of an active prosthetic joint that can dynamically adapt to changing terrain and gait needs is a limiting factor in attaining adequate comfort and mobility in below-knee amputees. Powered ankle prostheses can adapt to some extent, but the rigidity and power required during the gait are usually varying depending on the activity pursued by the individual. Such unknown, varying requirement cannot be addressed through standard control techniques. One of the key steps in the development of these active prosthetic feet is the generation of adaptive torque profiles to drive the ankle joint in

response to variations in the human locomotion. The design should also provide necessary energy return to significantly reduce the metabolic energy consumption during locomotion (Versluys et al., 2009). In an effort to achieve these goals, bionic feet such as Proprio Foot (Össur), BiOM (iWalk, 2012), SPARKy (Hitt et al., 2009), PPAMs (Versluys et al., 2008) have been equipped with active components that can modify the dynamic characteristics of the prosthetic ankle joints. It is noted that the ankle joints currently available are typically controlled using classical control techniques. Once the controller is tuned, its parameters are usually fixed irrespective of any changes in gait. Adaptive control strategies can account for changes in gait. However, such adaptive strategies have to overcome the challenges due to lack of information on gait and interaction between the foot and the ground as well as the interaction between the prosthetic socket and the residual limb. In the absence of such information, optimization of the performance of the controller becomes a very challenging task and requires the use of new design strategies such as learning-based control.

Mathematical models and experimental data can be effectively combined to generate forward

simulation of both normal and pathological gaits (Millard et al., 2008; Peasgood et al., 2007; Thelen and Anderson, 2006).

Figure 1 shows the diagram of the control-based approach which concentrates on generating suitable control signals to drive the model dynamics along desired trajectories obtained from the analysis of human gait (Xiang et al., 2010). In this framework, different methods of generating the joint torque can be analytically evaluated and the overall performance can be improved by feedback modification. Similarly, simulation frameworks which combine mathematical gait model and experimental data can be used to study the effect of prosthesis on kinematic behaviours and other aspects of amputee locomotion (Pejhan et al., 2008; Brugger and Schemiedmayer, 2003). Such simulation enables a quick evaluation of the performance of the prosthetic device under different operating conditions and extend the understanding of the prosthetic ankle-foot systems (Hansen, 2005). However, due to the complex interaction between the gait and the ground and the unknown intent of the user, it is not easy to guarantee efficient gait or robustness in performance. Therefore, a suitable control strategy that permits online adaptation to variations in gait while guaranteeing robust performance and improved efficiency has to be developed.

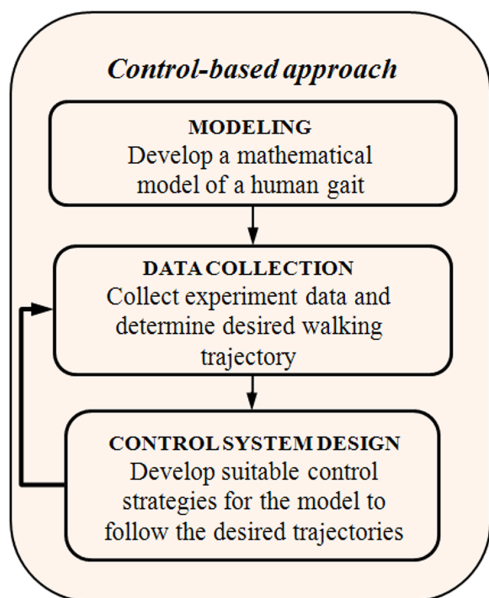


Figure 1: Control-based approach to the modelling and control of human gait.

In this paper, the use of Direct Neural Dynamic Programming-based control (Si and Wang, 2001) of

an active prosthetic ankle joint is evaluated. DNDP has been shown to be suitable for control of complex nonlinear systems with unknown dynamics and disturbances (Lu et al., 2008; Enns and Si, 2003). Furthermore, this approach also tries to minimize the long-term cost function in the sense of Bellman’s principle of optimality (dynamic programming). With these properties, DNDP appears to be a good candidate for a challenging task such as control of a prosthetic ankle. In order to apply this control technique, this paper addresses issues such as gait dynamics formulation, desired behaviours of the ankle joint during gait, control strategies, and long-term gait-related performance indices. In addition, augmented training rules are proposed to provide robustness against the foot-ground interaction disturbance. This is the first attempt in applying such a real-time adaptation scheme in learning the gait parameters and adjusting the control output to improve the gait and eliminate the asymmetry in gait between the amputated and the intact sides of the individual while enabling the individual to have a more active lifestyle. This will have enormous impact on the quality of life as well as the long-term health of people with below-knee amputation.

The rest of this paper is organized as follows. Section 2 describes the system models which include the dynamics of the gait and ground-foot interaction. Section 3 and 4 gives detailed information on kinematic pattern generation and control structures, respectively. Simulation setup with result discussions are presented in Section 5 and the conclusions of the investigation are presented in Section 6.

2 DYNAMICAL MODELS

2.1 Gait Model

The dynamic model in the sagittal plane of the residual limb of a unilateral below-knee amputee is considered in this study. This link-segment model includes 3 revolute joints: the hip joint connecting the biological thigh with the upper part of the human body; the knee joint connecting the biological thigh with the residual limb/artificial shank, and the prosthetic ankle joint connecting the artificial shank with the prosthetic foot. The action of the human muscles and ligaments that control the hip and knee joints are represented by the torques at those biological joints. At the prosthetic ankle joint, an externally powered actuator generates a torque to manipulate the angular position of the ankle.

The kinematic and dynamic relationship of the link-segment model in Figure 2 is obtained using the Euler-Lagrange formulation (Amirouche, 1992) following assumptions similar to those in Section 5.0.1 and Section 8.0.1 of (Winter, 2009). The interaction between the residual limb and the socket to which the prosthetic foot is connected is ignored and the residual-biological-artificial shank is considered rigid. The equations that govern the dynamics of the overall human-prosthetic system can be expressed as follows:

$$M(\theta)\ddot{\theta} + V(\theta, \dot{\theta})\dot{\theta} + G(\theta) + F(\theta)\ddot{a}_H = \tau + DF_{GRF} \quad (1)$$

where $\theta = [\theta_1 \ \theta_2 \ \theta_3]^T$ are joint angles (rad), $\dot{\theta} = [\dot{\theta}_1 \ \dot{\theta}_2 \ \dot{\theta}_3]^T$ are joint angular velocities (rad/s), and $\ddot{\theta} = [\ddot{\theta}_1 \ \ddot{\theta}_2 \ \ddot{\theta}_3]^T$ are joint angular accelerations (rad/s²); $\ddot{a}_H = [\ddot{x}_H \ \ddot{y}_H]^T$ are the hip acceleration (m/s²), $\tau = [\tau_1 \ \tau_2 \ \tau_3]^T$ are components of joint torques (Nm), and

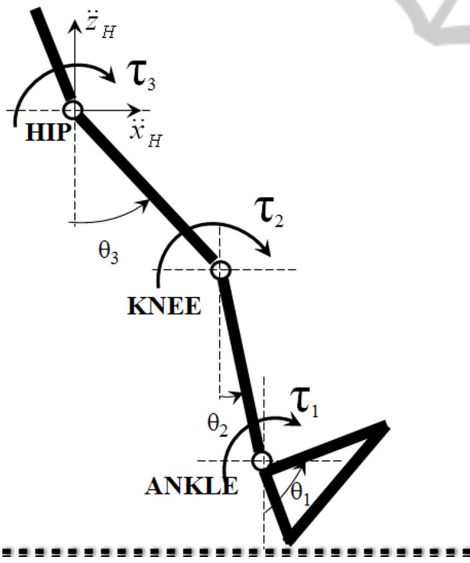


Figure 2: Link-segment representation of the residual limb with a prosthetic ankle joint.

$F_{GRF} = [F_X \ F_Z]^T$ are horizontal and vertical components of the ground reaction force (N). The nonlinear terms in (1) include the inertia matrix $M(\theta)$, the Coriolis and Centripetal term $V(\theta, \dot{\theta})$, the gravity term $G(\theta)$, the coefficient matrix $F(\theta)$ representing the translation of the hip, and the

coefficient matrix $D(\cdot)$ that represents the effect of the ground reaction force on the dynamic of each joint. Among these components, the ground reaction forces play a very important role and will be described in the subsequent section.

2.2 Ground Reaction Force

According to Winter (Winter, 2009), there are three forces acting on the link-segment model of the human gait: gravitational force, ground reaction force, and muscle and ligament forces. In the depicted gait model, the gravitational force is represented by the nonlinear term $G(\theta)$ whereas the force generated by the muscles and ligaments are replaced by the torque applied at the biological hip and knee joints. The ground reaction forces are generated during the gait as the result of interaction between the foot and the ground. Such reaction forces are then transferred up to the ankle, knee, and hip joints with the effect of altering the joint angular positions. Because the interaction between the foot and the ground is very complicated, it is very hard, if not impossible to exactly measure the ground reaction force without using carefully designed gait lab and force transducers (Winter, 2009). On the other hand, the ground reaction force (GRF) cannot be ignored during the simulation of the human gait (Wojtyra, 2003; Peasgood et al., 2007). Therefore, the following widely used model is selected to represent the ground reaction force for the experimental simulations used in this study (Peasgood et al., 2007; Millard et al., 2008).

$$F_Z = k(z_{PEN})^e + Step(y, 0, 0, d_{max}, c_{max})\dot{z}_{PEN} \quad (2)$$

$$F_X = \mu F_Z \operatorname{sgn}(\dot{x}_{COP}) \quad (3)$$

In this GRF model, F_Z and F_X are vertical and horizontal force components (N); z_{PEN} , \dot{z}_{PEN} are the penetration (m) and penetration rate (m/s); k, e are spring coefficient (N/m) and spring exponent; c_{max} is the maximal damping coefficient (N/(m/s)); d_{max} is the maximal damping penetration (mm); μ is the friction coefficient; and \dot{x}_{COP} is the horizontal velocity of the contact point with respect to the ground (m/s). Detailed descriptions of the parameters of this model can be found in (Peasgood et al., 2007).

The use of this ground reaction force model is more realistic than the rigid contact approach because it can simulate the viscous-elastic behaviour of the foot-ground interaction (Bruneau and

Ouezdou, 1997). The penetration of the foot into the ground is modified from (Marhefka and Orin, 1999). Because the ground reaction force can neither be measured exactly nor be ignored, the ground reaction force is treated as external disturbance to the gait dynamics during the simulation of the control strategy.

3 KINEMATIC PATTERN GENERATION

In order to study the effectiveness of the DNDP-based control strategy, the behaviour of the overall human-prosthetic system under different gait conditions has to be investigated. The different gaits are represented by kinematic patterns of angular positions, velocities, and accelerations of each of the joints. These quantities are obtained from the gait lab database (Winter, 1991) from real human subjects and are widely used in simulation of human gait. From the gait lab database, the analytical forms of the desired joint trajectories in time domain are generated to allow multi-step simulation of the model (Millard et al., 2008).

The desired joint trajectories of the hip, knee, and ankle joints, and the vertical Cartesian trajectory of the hip joint are approximated by five-term Fourier series as in equation below. The horizontal Cartesian trajectory of the hip joint is approximated by the sum of a first order polynomial (linear) and five-term Fourier series as in equation below. Given these analytical form trajectories, the required first and second order derivatives can be calculated without introducing any discontinuities in the model during simulation.

4 CONTROL STRUCTURE

Figure 3 shows the structure of the controller used in this study. The control structure can be divided into the control for the biological joints (hip and knee joints), and control for the prosthetic ankle joint.

4.1 Control of the Hip and Knee Joints

For the biological hip and knee joints, it is assumed that below-knee amputees are able to adjust their muscle activities to generate enough torques to manipulate these joints and maintain normal gait despite possible control efforts at the prosthetic

ankle joint. For that reason, ideal computed torque control is applied at the hip and knee joints. These ideal torques are computed assuming that the (noisy) joint angles, angular velocities, and angular accelerations, as well as the nonlinear terms in (1) are known. Such control inputs have the same structure as the ideal computed torque control for robot manipulators (Lewis et al., 1999).

Equations (8) and (9) describe the ideal computed torque control applied at the biological hip and knee joints during simulation of the model, in which $e_i = (\theta_{ir} - \theta_i)$ and $\dot{e}_i = (\dot{\theta}_{ir} - \dot{\theta}_i)$ are tracking errors of each joint, $\ddot{\theta}_{ir}$ is a desired angular acceleration of each joint, $K_{Di} > 0, K_{Pi} > 0$ are design parameters.

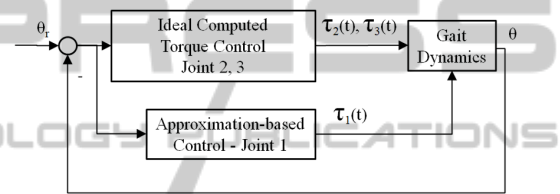


Figure 3: Control structure with ideal computed torque control at hip and knee joints, and approximation-based control at the prosthetic ankle joint.

4.2 Control of the Ankle Joint

The angular position of the prosthetic ankle joint can be controlled by an external actuator. In this model, the dynamics of the actuator are ignored and only the torque produced at the prosthetic joint is considered. In contrast to the ideal joint controllers used for the biological hip and knee joints, the actuator at the prosthetic ankle joint is assumed to have access to only the actual ankle angle and angular velocity. Such quantities could be measured by using a rotational encoder and gyroscope mounted on the prosthetic foot. Therefore, the torque produced by an external actuator could be a function of the ankle angle, the ankle angular velocity, and the tracking error between these quantities and their desired kinematic patterns as follows:

$$\tau_1 = f(\theta_1, \dot{\theta}_1, e_1, \dot{e}_1) \quad (4)$$

where e_1 and \dot{e}_1 are tracking errors of the ankle angle and ankle angular velocities as defined above.

The filtered tracking error is used as in (Lewis et al., 1999):

$$r_1 = \dot{e}_1 + \lambda_1 e_1 \quad (5)$$

$$\{\theta_{3r}(t), \theta_{2r}(t), \theta_{1r}(t), z_{Hr}(t)\} = a_0 + \sum_{k=1}^5 a_i \cos(kwt) + b_i \sin(kwt) \quad (6)$$

$$x_{Hr}(t) = k_0 t + m_0 + c_0 + \sum_{k=1}^5 c_i \cos(kwt) + d_i \sin(kwt) \quad (7)$$

$$\begin{aligned} \tau_2 = & M_{21}(\ddot{\theta}_{1r} + K_{D1}\dot{e}_1 + K_{P1}e_1) + M_{22}(\ddot{\theta}_{2r} + K_{D2}\dot{e}_2 + K_{P2}e_2) + M_{23}(\ddot{\theta}_{3r} + K_{D3}\dot{e}_3 + K_{P3}e_3) \\ & + V_{21}\dot{\theta}_1 + V_{22}\dot{\theta}_2 + V_{23}\dot{\theta}_3 + G_2 + F_{21}\ddot{x}_H + F_{22}\ddot{z}_H - D_{21}F_X - D_{22}F_Z \end{aligned} \quad (8)$$

$$\begin{aligned} \tau_3 = & M_{31}(\ddot{\theta}_{1r} + K_{D1}\dot{e}_1 + K_{P1}e_1) + M_{32}(\ddot{\theta}_{2r} + K_{D2}\dot{e}_2 + K_{P2}e_2) + M_{33}(\ddot{\theta}_{3r} + K_{D3}\dot{e}_3 + K_{P3}e_3) \\ & + V_{31}\dot{\theta}_1 + V_{32}\dot{\theta}_2 + V_{33}\dot{\theta}_3 + G_3 + F_{31}\ddot{x}_H + F_{32}\ddot{z}_H - D_{31}F_X - D_{32}F_Z \end{aligned} \quad (9)$$

in which $\lambda_i > 0$ is the design parameter.

With the introduction of the filtered tracking error, the dynamics of the ankle joint

$$\begin{aligned} M_{11}\ddot{\theta}_1 + M_{12}\ddot{\theta}_2 + M_{13}\ddot{\theta}_3 + V_{11}\dot{\theta}_1 + V_{12}\dot{\theta}_2 + V_{13}\dot{\theta}_3 \\ + G_1 + F_{11}\ddot{x}_H + F_{12}\ddot{z}_H = \tau_1 + D_{11}F_X + D_{12}F_Z \end{aligned} \quad (10)$$

can be written in term of the filtered tracking error as follows:

$$M_{11}\dot{r}_1 = -V_{11}r_1 + f_1(x) - \tau_1 \quad (11)$$

with the nonlinear term $f_1(x)$ is given as:

$$\begin{aligned} f_1(x) = & M_{11}(\ddot{\theta}_{1r} + \lambda_1\dot{e}_1) + M_{12}(\ddot{\theta}_{2r} - \dot{r}_2 + \lambda_2\dot{e}_2) + \\ & M_{13}(\ddot{\theta}_{3r} - \dot{r}_3 + \lambda_3\dot{e}_3) + V_{11}(\dot{\theta}_{1r} + \lambda_1e_1) + \\ & V_{12}(\dot{\theta}_{2r} - \dot{r}_2 + \lambda_2e_2) + V_{13}(\dot{\theta}_{3r} - \dot{r}_3 + \lambda_3e_3) + \\ & G_1 + F_{11}\ddot{x}_H + F_{12}\ddot{z}_H - D_{11}F_X - D_{12}F_Z \end{aligned} \quad (12)$$

This nonlinear term, especially the contribution of the acceleration of the hip joint ($F_{11}\ddot{x}_H + F_{12}\ddot{z}_H$) and the moments generated by the ground reaction force ($-D_{11}F_X - D_{12}F_Z$), is unknown and difficult to compute. The nonlinearity of this function is further increased in multi-step simulation due to the fact that the ground reaction forces only affect the gait dynamics during the stance phases when the residual limb is contacting the ground. However, these forces are not present during the swing duration. To overcome these difficulties, this nonlinear function will be approximated in the DNDP-based framework.

Given the approximation of the nonlinear term $f_1(x)$, the approximation-based control signal will be selected as follows:

$$\tau_1 = \hat{f}_1(x) + K_{V1}r_1 \quad (13)$$

with $\hat{f}_1(x)$ is an approximation of $f_1(x)$ and $K_{V1}r_1$ is a Proportional-Derivative (PD) control term, and r_1 is the filtered tracking error in (5).

4.2.1 DNDP-based Control Structure

The DNDP-based control structure comprises of two neural networks: critic network and action network. The critic network is responsible to generate an approximate of the long-term cost function which satisfies the Bellman's principle of optimality. The action network is responsible for generating a control signal which leads to the optimization of the approximated long-term cost (or output of the critic network). Figure 4 presents the two-network configuration of the DNDP-based control. The next section will provide detailed information about elements in Figure 4.

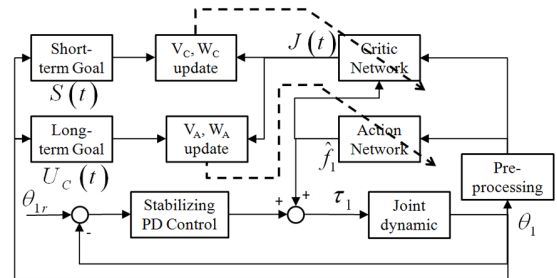


Figure 4: DNDP-based control of the prosthetic ankle joint.

4.2.2 Detailed Implementation

The critic network approximates the discounted long-term cost which is represented as the weighted sum of the short-term (instantaneous) cost as follows:

$$\begin{aligned} L(t) &= S(t+1) + \alpha S(t+2) + \alpha^2 S(t+3) + \dots \\ &= S(t+1) + \alpha L(t+1) \end{aligned} \quad (14)$$

with α is the discount factor.

Because the critic network is responsible for calculation of the quantity $J(t)$ as an approximation of the long-term cost function $L(t)$, the backpropagation error is defined as:

$$e_C(t) = \underbrace{[J(t-1) - S(t)]}_{\text{TARGET}} - \underbrace{\alpha J(t)}_{\text{CURRENT OUTCOME}} \quad (15)$$

where $S(t)$ is the instantaneous cost at time t (short term cost).

Inputs to the critic network are:

$$x_C = [e_1 \quad \dot{e}_1 \quad \theta_1 \quad \dot{\theta}_1 \quad \hat{f}_1(x_A)]^T \quad (16)$$

and the critic network output is the approximation of the long-term cost function defined in equation (14):

$$\begin{aligned} J &= \hat{W}_C^T \hat{\sigma}_C(\hat{V}_C^T x_C) \\ &= \sum_{i=1}^{L_C} \hat{W}_C^T(1,i) \hat{\sigma}_C \left(\sum_{j=1}^{N_C} \hat{V}_C^T(i,j) x_C(j,1) \right) \end{aligned} \quad (17)$$

with L_C is the number of nodes in the hidden layer, and $N_C = 5$ is the number of inputs to the critic network.

Weights of the critic network are trained as follows:

$$\dot{\hat{W}}_C = \alpha F_C e_C \hat{\sigma}_C - k_C F_C \|e_C\|_2 \hat{W}_C \quad (18)$$

$$\dot{\hat{V}}_C = \alpha G_C e_C x_C \hat{W}_C^T \hat{\sigma}'_C - k_C G_C \|e_C\|_2 \hat{V}_C \quad (19)$$

in which α is the discount factor, F_C, G_C, k_C are design parameters, and $\hat{\sigma}'_C$ is the Jacobian matrix defined as:

$$\hat{\sigma}'_C = \frac{\partial \hat{\sigma}_C(\hat{V}_C^T x_C)}{\partial (\hat{V}_C^T x_C)}$$

In this design, the action network approximates the unknown nonlinear function $f_1(x)$. In general, the action network is responsible for generating a control which results in the optimization of the long-term cost function, i.e. the output of the critic network. Therefore, the backpropagation error of the

action network is given as follows:

$$e_A(t) = \underbrace{U_C(t)}_{\text{TARGET}} - \underbrace{J(t)}_{\text{CURRENT OUTCOME}} \quad (20)$$

where $U_C(t)$ is an ultimate control goal, or the target for the long-term cost approximate $J(t)$.

Inputs to the action network are:

$$x_A = [e_1 \quad \dot{e}_1 \quad \theta_1 \quad \dot{\theta}_1]^T \quad (21)$$

and structure of the action network is as follows:

$$\begin{aligned} \hat{f}_1 &= \hat{W}_A^T \hat{\sigma}_A(\hat{V}_A^T x_A) \\ &= \sum_{i=1}^{L_A} \hat{W}_A^T(1,i) \hat{\sigma}_A \left(\sum_{j=1}^{N_A} \hat{V}_A^T(i,j) x_A(j,1) \right) \end{aligned} \quad (22)$$

in which L_A is the number of nodes in the hidden layer, and $N_A = 4$ is the number of inputs to the action network.

Weights of the action network are trained as follows:

$$\begin{aligned} \dot{\hat{W}}_A &= F_A e_A \hat{\sigma}_A \hat{V}_{CA} \hat{\sigma}'_C \hat{W}_C - F_A \hat{\sigma}'_A \hat{V}_A^T x_A r_1 \\ &\quad - k_A F_A \|e_A\|_2 \hat{W}_A \end{aligned} \quad (23)$$

$$\dot{\hat{V}}_A = G_A e_A x_A \hat{V}_{CA} \hat{\sigma}'_C \hat{W}_C \hat{W}_A^T \hat{\sigma}'_A - k_A G_A \|e_A\|_2 \hat{V}_A \quad (24)$$

in which \hat{V}_{CA} is obtained from \hat{V}_C to map from $\hat{f}_1(x_A)$ to the hidden node output, F_A, G_A, k_A are design parameters, and $\hat{\sigma}'_A$ is the Jacobian matrix defined as:

$$\hat{\sigma}'_A = \frac{\partial \hat{\sigma}_A(\hat{V}_A^T x_A)}{\partial (\hat{V}_A^T x_A)}$$

Compared to the weight updating rules in (Si and Wang, 2001), it is noted that the last terms in (18), (19), (23), and (24) provide robustness against the disturbances generated by the ground reaction forces which affect the gait dynamics during stance phase of the gait cycle. Finally, the DNDP-based control is given as in (13).

4.2.3 Selection of the Short-term (Instantaneous) Performance Index (Cost) and the Ultimate Control Goal

The short-term (or instantaneous) cost at each time step is calculated as follows:

$$S(t) = -\frac{1}{2} \left(\frac{\theta_{1r}(t) - \theta_1(t)}{\theta_{1M}} \right)^2 - \frac{1}{2} \left(\frac{\dot{\theta}_{1r}(t) - \dot{\theta}_1(t)}{\dot{\theta}_{1M}} \right)^2 \quad (25)$$

where $\{\theta_1(t), \dot{\theta}_1(t)\}$, $\{\theta_{1r}(t), \dot{\theta}_{1r}(t)\}$ and $\{\theta_{1M}, \dot{\theta}_{1M}\}$ are actual, desired, and maximal values of the ankle joint angular position and velocity. This selection relates to the gait efficiency in the way that if the prosthetic ankle joint can perform as closed as possible to the biological ankle, then the hip and knee joints will not have to modify their behaviours. As the result, the overall human-prosthetic system can provide normal gait.

The ultimate control goal is selected as $U_C(t) = 0$ which implies the maximization of the long-term cost function which is the weighted sum of the short-term cost.

5 NUMERICAL STUDY

In this section, the performance of the DNDP-based control is evaluated through simulation of the developed link-segment model with the presence of measurement/actuator noises and variations in walking speed.

5.1 Simulation Setup

Kinematic data collected from human subjects during walking with different cadences (natural, fast, slow) in the gait lab (Winter, 1991) is converted to represent the kinematic patterns for the human-prosthetic dynamic model in corresponding gaits with normal, fast, and slow walking speed. For multi-step simulation of the gait dynamic (1), the kinematic patterns are approximated by using equations (6) and (7).

Design parameters for the ideal computed torque controls at the hip and knee joints are $K_P = 10$ and $K_D = 5$. At the ankle joint, the DNDP-based control is generated by an action network with 4 nodes at the input layer, 8 nodes in the hidden layer, and 1 node in the output layer. The critic network has 5 nodes at the input layer, 10 nodes at the hidden layer, and 1 node at the output layer. Both networks use sigmoid activation functions and are fully connected with randomly initialized weights in the range $[-1, 1]$. Other design parameters include the discount factor $\alpha = .95$ and PD control with $K_{V1} = 5$ and $\lambda_1 = 10$. The unknown nonlinear function

$f_1(x)$ is approximated by (22). The critic network and action network weights are updated using (18)-(19) and (23)-(24), respectively. Equation (25) is used to calculate the short-term cost at each time step.

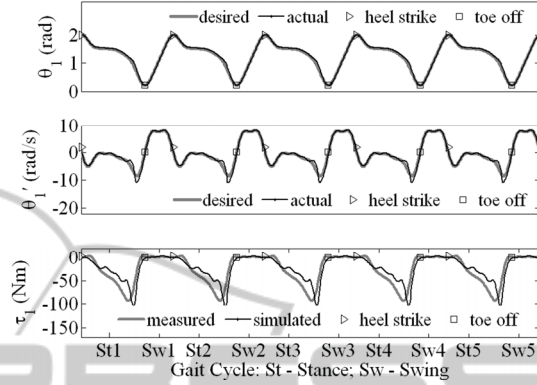


Figure 5: Tracking performance of the DNDP-based control during normal speed under ideal conditions.

5.2 Ideal Condition

In this ideal condition, the model is simulated during a gait including 20 steps of normal speed without any measurement and actuator noises. The tracking performance of the ankle joint and DNDP-based torque action for 5 steps are shown in Figure 5. It is observed that both the ankle position and angular velocity can follow their desired trajectories with small errors. More interestingly, the DNDP-based ankle torque generated during simulation of the model is very similar to the biological ankle torque measured from human subjects during gait lab testing (Winter, 1991).

5.3 Effect of Measurement and Actuator Noises

Uniformly distributed measurement noises are added to the ankle position and angular velocity. Torque output generated for the ankle joint is also added with uniformly distributed actuator noise as follows:

$$\begin{aligned} \theta_1 &= \theta_1 + \rho_{\theta} \theta_1 \\ \dot{\theta}_1 &= \dot{\theta}_1 + \rho_{\dot{\theta}} \dot{\theta}_1 \\ \tau_1 &= \tau_1 + \rho_{\tau} \tau_1 \end{aligned} \quad (26)$$

where ρ_{θ} , $\rho_{\dot{\theta}}$, and ρ_{τ} are in the range $[-2\%, 2\%]$ (or $[-5\%, 5\%]$). The model is simulated with 20

steps of normal walking speed and increasing measurement and/or actuator noises (see Table 1).

Table 1: Long-term cost during 20 steps of normal walking speed and increasing measurement/actuator noises.

| Noise | PD | FLNN | DNDP |
|--|-------|-------|-------|
| 2% measurement noise | 0.715 | 0.239 | 0.075 |
| 5% measurement noise | 3.96 | 2.003 | 0.118 |
| 5% measurement noise and 2% actuator noise | 3.961 | 2.079 | 0.120 |
| 5% measurement noise and 5% actuator noise | 3.966 | 2.336 | 0.130 |

PD – Proportional-Derivative control

FLNN –Feedback Linearization Neural Network control

For the comparison purpose, the model is simulated with other types of control at the ankle joint, including Proportional-Derivative control (PD) and direct Feedback Linearization-based multilayer Neural Network control (FLNN). Ideal computed torque controls are still used at the hip and knee joints given the assumption on the human ability in generating normal gait. The average long-term cost function as calculated by (14) is reported in Table 1. It can be seen that as the measurement/actuator noises increase, the DNDP-based control outperforms other control methods by producing robust tracking performance with lower long-term cost.

5.4 Effect of Variations in Walking Speed

Similar setups to Section 5.3 are repeated here to evaluate the performance of the DNDP-based control in the presence of variations in walking speed. The model is simulated with 5% measurement noise, 5% actuator noise, and 4 different walking setups (see Table 2).

Table 2: Long-term cost with 5% measurement noise, 5% actuator noise, and combinations of different walking speeds.

| Number of steps | PD | FLNN | DNDP |
|-----------------------------|-------|-------|-------|
| 10 normal + 10 fast | 2.140 | 0.567 | 0.100 |
| 10 normal + 10 slow | 3.910 | 1.915 | 0.106 |
| 10 normal + 5 fast + 5 slow | 2.233 | 0.461 | 0.082 |
| 10 normal + 5 slow + 5 fast | 2.206 | 0.490 | 0.084 |

Again, despite the variations in walking speed, the DNDP-based control is still able to provide lower long-term performance cost compared to other control strategies.

6 CONCLUSIONS

The performance of a model-free Direct Neural Dynamic Programming-based controller for a prosthetic ankle joint was investigated in this paper. Issues such as gait dynamics formulation, desired ankle joint behaviours, control strategies, and long-term gait-related efficiency were addressed in order to implement the DNDP-based control approach. We augmented the original training rules with additional terms to provide robustness against the disturbance generated by the ground reaction force. Results of the simulation study indicate that the DNDP-based control is stable, robust to measurement/actuator noises and variations in walking speeds, and improves the overall performance of the prosthetic ankle. It is also observed that the generated ankle torque is similar to the torque measured from biological ankle during gait testing. The results of this study serve as a starting point for the development of intelligent ankle prosthesis. The authors are currently pursuing research on adaptive determination of gait using biofeedback signals measured from below-knee amputees and implementation of the DNDP-based control strategy on actual prosthetic ankle joint.

REFERENCES

Amirouche, F. M. L. 1992. *Computational Methods in Multibody Dynamics*, Prentice Hall.

Brugger, P. & Schemiedmayer, H.-B. 2003. Simulating prosthetic gait - lessons to learn. *Proceedings in Applied Mathematics and Mechanics*, 3, 64-67.

Bruneau, O. & Ouedzou, F. B. 1997. Compliant contact of walking robot feet. *3rd ECPD International Conference on Advanced Robotics*. Bremen, Germany.

Enns, R. & Si, J. 2003. Helicopter trimming and tracking control using direct neural dynamic programming. *IEEE Transactions on Neural Networks*, 14, 929-939.

Hansen, A. H. 2005. Scientific methods to determine functional performance of prosthetic ankle-foot systems. *Journal of Prosthetics and Orthotics*, 17, 23-29.

Hitt, J., Sugar, T., Holgate, M., Bellman, R. & Hollander, K. 2009. Robotic transtibial prosthesis with biomechanical energy regeneration. *International Journal of Industrial Robot*, 36, 441-447.

iWalk. 2012. *Bionic Technology with Powered Plantar Flexion* [Online]. Available: <http://www.iwalkpro.com/Prosthetists.html> [Accessed Aug. 28th 2012].

Lewis, F. L., Jagannathan, S. & Yesilderek, A. 1999. *Neural network control of robot manipulators and nonlinear systems*, London, UK, Taylor & Francis.

- Lu, C., Si, J. & Xie, X. 2008. Direct heuristic dynamic programming for damping oscillations in a large power system. *IEEE Transactions on Systems, Man, and Cybernetics - Part B: Cybernetics*, 38, 1008-1013.
- Marhefka, D. W. & Orin, D. E. 1999. A compliant contact model with nonlinear damping for simulation of robotic systems. *IEEE Transactions on Systems, Man, and Cybernetics - Part A: Systems and Humans*, 29, 566-572.
- Millard, M., McPhee, J. & Kubica, E. 2008. Multi-step forward dynamic gait simulation. *Computational Methods in Applied Sciences*, 12, 25-43.
- Össur. *Proprio Foot* [Online]. Available: <http://www.ossur.com/?PageID=12704> [Accessed Nov. 5th 2012].
- Peasgood, M., Kubica, E. & McPhee, J. 2007. Stabilization of a dynamic walking gait simulation. *ASME Journal of Computational and Nonlinear Dynamics*, 2, 65-72.
- Pejhan, S., Farahmand, F. & Parnianpour, M. 2008. Design optimization of an above-knee prosthesis based on the kinematics of gait. *30th Annual International IEEE EMBS Conference*. Vancouver, British Columbia, Canada.
- Si, J. & Wang, Y.-T. 2001. On-line learning control by association and reinforcement. *IEEE Transactions on Neural Networks*, 12, 264-276.
- Thelen, D. G. & Anderson, F. C. 2006. Using computed muscle control to generate forward dynamic simulations of human walking from experiment data. *Journal of Biomechanics*, 39, 1107-1115.
- Versluys, R., Beyl, P., Damme, M. V., Desomer, A., Ham, R. V. & Lefeber, D. 2009. Prosthetic feet: state-of-the-art review and the important of mimicking human ankle-foot biomechanics. *Disability and Rehabilitation: Assistive Technology*, 4, 65-75.
- Versluys, R., Desomer, A., Lenaerts, G., Damme, M. V., Beyl, P., Perre, G. V. d., Peeraer, L. & Lefeber, D. 2008. A pneumatically powered below-knee prosthesis: design specifications and first experiments with an amputee. *2nd Biennial IEEE/RAS-EMBS International Conference on Biomedical Robotics and Biomechanics*. Scottsdale, AZ, USA.
- Winter, D. A. 1991. *The biomechanics and motor control of human gait: normal, elderly and pathological*, Waterloo, Ontario, Canada, University of Waterloo Press.
- Winter, D. A. 2009. *Biomechanics and motor control of human movement*, Hoboken, N. J., Wiley.
- Wojtyra, M. 2003. Multibody simulation model of human walking. *Mechanics Based Design of Structures and Machines*, 31, 357-379.
- Xiang, Y., Arora, J. S. & Abdel-Malek, K. 2010. Physics-based modeling and simulation of human walking: a review of optimization-based and other approaches. *Medical and Bioengineering Application*, 42, 1-23.